

UDK: 53.086, 622.785

Cavitation Resistance of the Material PA 3200 GF Produced by Selective Laser Sintering

**Marina B. Dojčinović¹, Olivera A. Erić Cekić^{2,3*)}, Igor Svetel²,
Snežana M. Ćirić-Kostić³, Nebojša M. Bogojević³**

¹Faculty of Technology and Metallurgy, University of Belgrade, Karnegijeva 4, 11000 Belgrade, Serbia

²Innovation Center of Mechanical Engineering Faculty, University of Belgrade, 11000 Belgrade, Serbia,

³Faculty of Mechanical and Civil Engineering in Kraljevo, University of Kragujevac, 36000 Kraljevo, Serbia

Abstract:

The present study focuses on the results of cavitation resistance research of samples obtained by the Selective Laser Sintering technology. The samples were made from polyamide powder reinforced with glass beads – PA 3200 GF. The laser-sintered samples were produced from 100% new and recycled powder mixed with 70% of new powder. The samples were tested under cavitation conditions using an ultrasonic vibration method with a stationary sample according to the ASTM G32 standard. Examination of the morphology of cavitation damage was investigated by scanning electron microscopy. The change in mass loss during different cavitation times was measured on the tested samples. The main objective of the research was to determine the validity of the application of the tested material in cavitation conditions.

Keywords: Polyamide powder; PA 3200 GF; Morphology; Cavitation rate; Selective laser sintering.

1. Introduction

Selective laser sintering technology (SLS) belongs to the powder bed fusion (PBF) additive technologies where the powder material is fused, point by point, using the energy of a laser or an electron beam. This additive manufacturing process depends on the large number of the parameters, such as laser power of the beam, laser spot size, hatch pattern, hatch speed, powder quality, etc. [1]. The main advantage of the PBF technology for production of parts from plastics and composites is possibility to produce parts with complex internal and external shapes without the need for fabrication of any kind of the supporting structure [2]. After fabrication the powder is cleaned from the parts using compressed air. After the cleaning of the powder, the parts are sand-blasted by glass spheres in order to improve the surface quality and remove the powder residues from the surface. In the SLS technology, the powder, by a recoater, is applied in a thin layer on the top surface of the working platform, and then a focused CO₂ laser is used to fuse the powder into the shape of a cross section of the part, and join to the previously created layer of the part. After the production of the cross

*) **Corresponding author:** olivera66eric@gmail.com

section is finished, the working platform is moved down for the thickness of a layer, and the process is repeated. In order to prevent the oxidation and ignition of the powder, the process of sintering is performed in the atmosphere of inert gas – e.g., nitrogen.

In spite of many materials which have been successfully used with selective laser sintering process, there is still a need to investigate new materials from the point of view of improved properties and qualities. The most researched polymer (polyamide PA) had become synonymous with SLS plastics. The material with best mechanical properties for producing functional parts by the SLS process is a nylon composite [3]. Glass beads-filled polyamide composites are characterized by excellent stiffness in combination with good elongation at break, high mechanical wear-resistance, low cost and widespread applications in automobile, aerospace and electrical industries [4].

Cavitation represents the formation, growth and implosion (collapse) of bubbles of steam or gas in a flowing fluid. The implosion of bubbles caused micro-jet and shock waves whose energy is either dissipated inside the liquid or absorbed by a solid contact surface [5-12].

Impacts caused by the collapse of cavitation bubbles may have amplitudes greater than the tensile strength of the material, and lead to elastic/ plastic deformations and surface damage and loss of material mass, i.e. cavitation erosion. During cavitation in collapsing bubbles, high temperatures and pressures are produced locally (approximately 5000 °C and 1000 bar) in a very short period of time (less than 1 μs) [13-16]. Cavitation resistance is a good indicator of material stability in extreme working conditions. Polyamide powder reinforced with glass beads, PA 3200 GF, have excellent mechanical properties and wear-resistance. Because of those properties, the cavitation resistance of this composite was evaluated in this paper in order to estimate the potential of employing glass-ceramics derived from CFA for the production of parts of industrial equipment.[17, 18]

2. Materials and Experimental Procedures

2.1. Synthesis and Characterization

Samples used for analysis in this study are produced using an EOS Formiga P100 machine (EOS GmbH, Krailling, Germany). The material used for samples was PA 3200 GF, which is a polyamide 12 filled with glass beads. The mechanical properties of the parts produced from this material, according to the EOS [19] are given in the Table I. The powder, with average grain size of 57 μm, can be reused after mixing with fresh powder. The samples produced from this material have density of the 1.22 g/m³, while the powder has a bulk density of the 0.63 g/m³. [20]

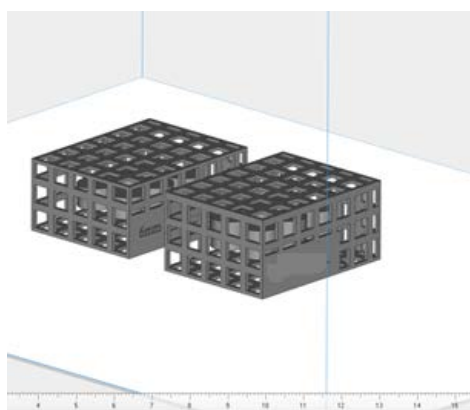


Fig. 1. Samples position and orientation in build volume.

Two sets of the samples were produced for the purposes of this study: the samples of the first set (A composite) were made using fresh powder, while the samples of the second set (B composite) were made using powder mixture containing 70% of the fresh powder and 30% of the already used powder. Each set of the samples contains 6 discs with diameter 10 mm and thickness 6 mm. During the production process, bases of the discs were parallel to plane of layers (i.e., normal to the build direction), as it is shown in the (Fig. 1.).

All samples were produced using standard parameter set for PA 3200 GF powder on Formiga P100 machine. The parameters for production samples were: layer thickness 0.1mm, laser power 21W, scanning speed 2500 mm/s, hatch distance 0.25mm and beam diameter 0.30 mm. Since the geometry of the samples was relatively simple, 3D models of discs were generated using Materialise Magics software package.

Tab. I. Mechanical properties of composite samples [19].

Mechanical properties	Value	Unit	Standard
Tensile modulus	3200 (464)	MPa (ksi)	EN ISO 527 (ASTM D638)
Tensile strength	51 (7397)	MPa (psi)	EN ISO 527 (ASTM D638)
Elongation at break	9	%	EN ISO 527 (ASTM D638)
Flexural modulus	2900 (421)	MPa (ksi)	EN ISO 178 (ASTM D790)
Flexural strength	73 (10588)	MPa (psi)	EN ISO 178 (ASTM D790)
Charpy - Impact strength	35	kJ/m ²	EN ISO 179
Charpy – Notched impact strength	5.4	kJ/m ²	EN ISO 179
Ball indentation hardness	98	N/mm ²	EN ISO 2039
Hardness, Shore D	80		ISO 868 (ASTM D2240)

2.2 Methods

2.2.1. Cavitation erosion testing

The ultrasonic vibration method (with a stationary sample) according to the ASTM G32 (ASTM Standard, 1992) standard [21] was used to determine the cavitation resistance of the samples. The ultrasonic vibration method is based on the creation and implosion of cavitation bubbles on the sample surface and measuring the loss of mass of the sample during the time of exposure to cavitation. The selection of characteristic parameters for testing was performed in accordance to the ASTM G32 standard: frequency of mechanical vibrations was 20 ± 0.2 kHz; amplitude of mechanical vibrations at the top of the concentrator was 50 ± 2 μ m; the gap between the test sample and the concentrator was 0.5 mm; water flow was 5–10 ml/s; water bath temperature was 25 ± 1 °C; sample exposure interval and total test time were: 30; 60; 90 and 120 min. Following each test period, the samples were dried and the mass of the samples was determined using an analytical balance with accuracy ± 0.1 mg. The results are shown in the mass loss versus time duration exposure diagram. The least squares method is used to construct straight lines whose slope specifies the cavitation rate.

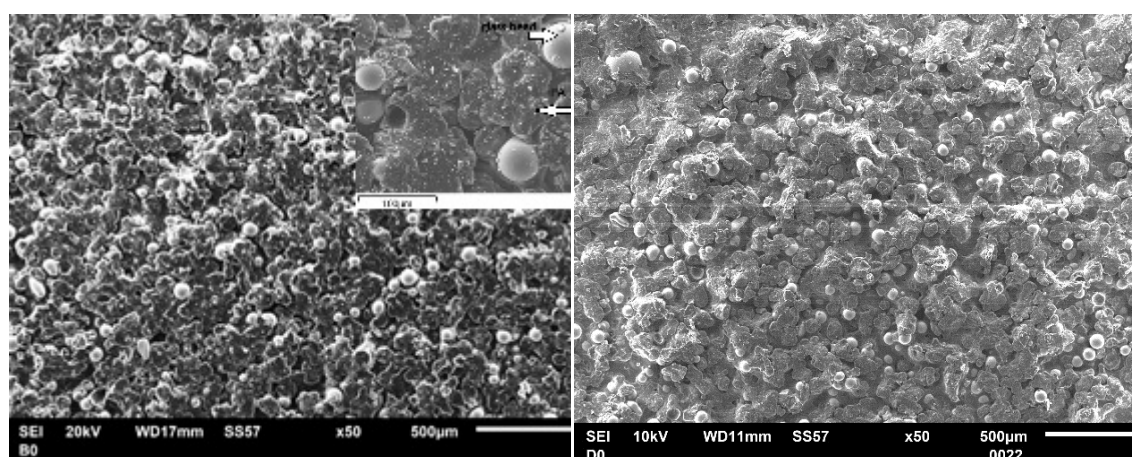
2.2.2 Microstructure and chemical characterization

The fracture surfaces were analyzed by a scanning electron microscope (SEM) JEOL JSM 6460 LV (JEOL, Tokyo, Japan) operated at 20 kV. Localized chemical analyses performed by energy-dispersive X-ray spectrometry (EDXS).

3. Results and Discussion

3.1. Microstructural analysis of PA 3200 GF material before the cavitation process

SEM microphotograph shows morphology of the A composite (Fig. 2a). The white regions are the glass beads, while the dark regions are the polyamide (PA) matrix. The inset figure is a high magnification micrograph of a selected region of the composite showing a glass particles (light regions indicated by white arrows) and the PA matrix (dark regions). Fig. 2b shows that the surface morphology has more pronounced peaks and valleys caused by the laser passage and many unmolten particles.



a) PA 3200 GF(100% fresh powder)
A composite

b) PA 3200 GF(70% fresh:30% used powder)
B composite

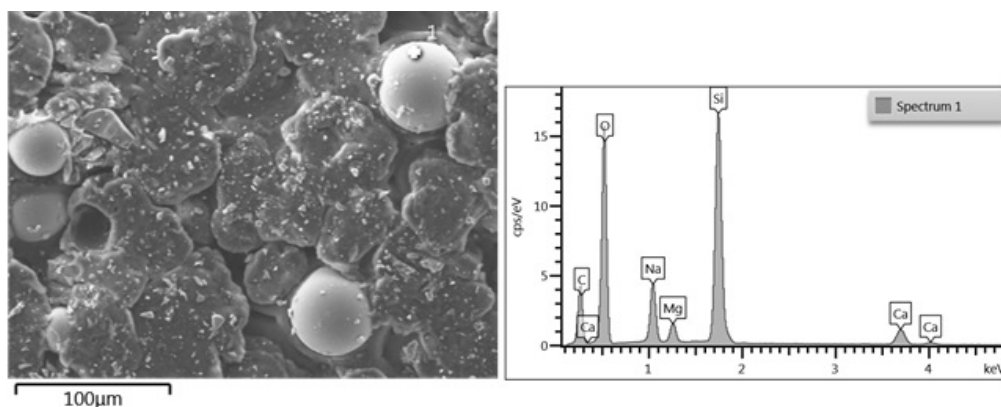
Fig. 2. SEM images of SLS-fabricated PA 3200 GF sample surfaces.

All specimens, with 100% fresh powder and specimens with 70% of the fresh powder and 30% of the already used powder were found to have less than 1% porosity. (Fig. 2a; Fig. 2b).

The SEM-EDX analysis of the PA 3200 GF sample (Fig. 3) revealed peaks of the present elements on the surface of PA 3200 GF sample, including oxygen, natrium, magnesium, silicium and calcium. In the PA 3200 GF with 100% fresh powder, there are glass beads in the PA matrix of different granulation.

Cavitation damage after 30 min

SEM micrographs after cavitation testing in water during 30 min are shown in Fig. 4a-b for A composite and Fig. 4c-d for B composite, respectively. Fig. 4a and Fig.4b show the presence of some broken glass beads in A composite and B composite.



Element	Wt %	Atomic %
O	51.22	64.42
Na	9.06	7.93
Mg	2.71	2.24
Si	31.81	22.79
Ca	5.19	2.61
Total:	100.00	100.00

Fig. 3. SEM-EDX analysis of the PA 3200 GF with 100% fresh powder.

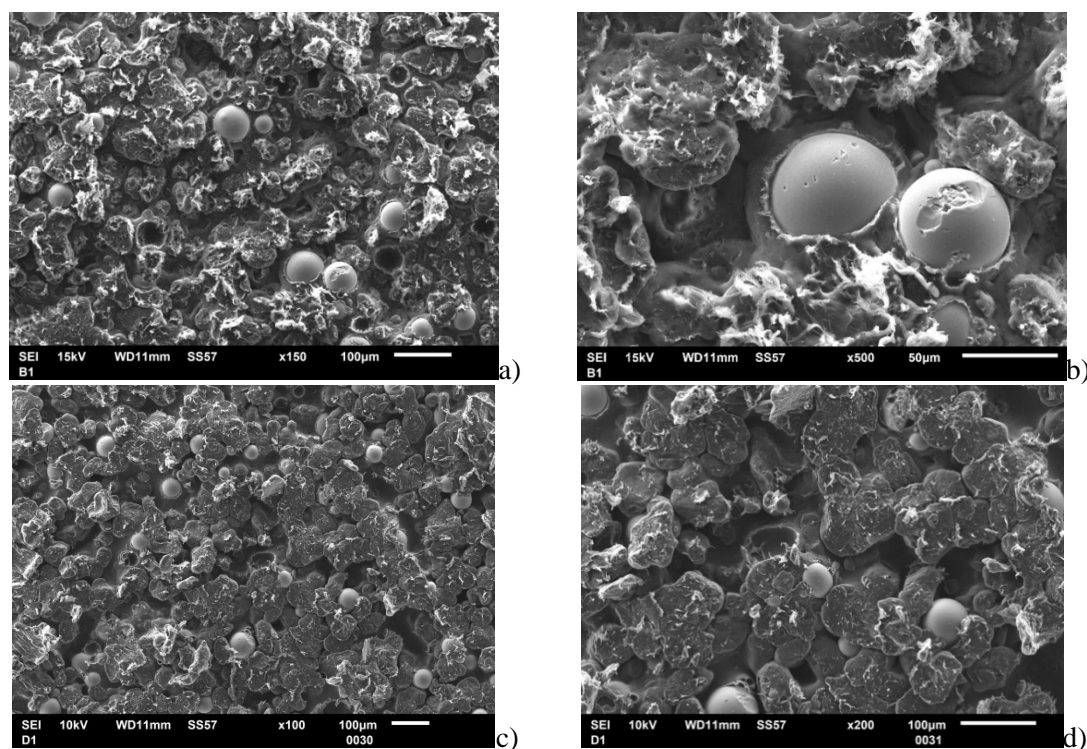


Fig. 4. SEM micrographs of (a; b) A composite and (c; d) B composite after cavitation testing in water during 30min.

It can be seen relatively large gaps were present between the layers and the glass particles (Fig. 4d). Cracks initiate at the interfaces of the melted polyamide matrix and the un-melted PA 3200 glass particle cores. The deformation and crack growth mainly occur within the melted polyamide matrix [22].

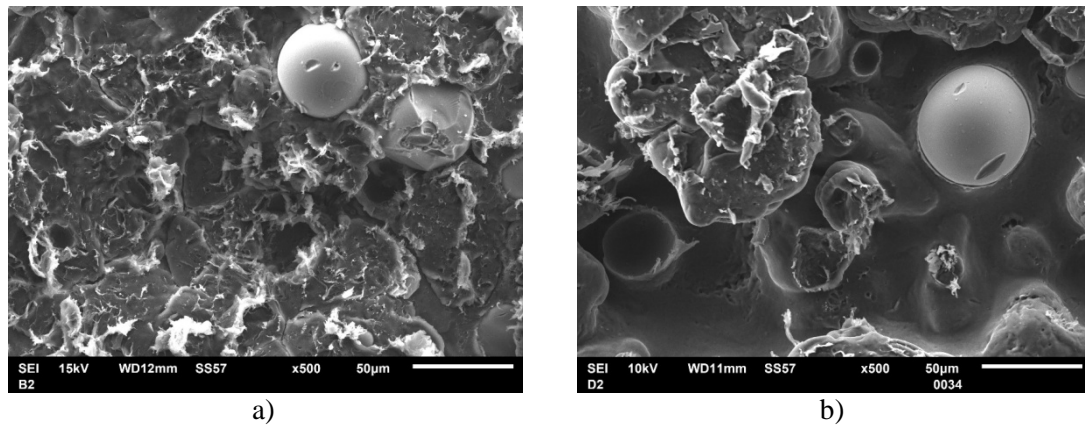


Fig. 5. SEM micrographs of (a) A composite and (b) B composite after cavitation testing in water after 60 min.

The damage morphology of the samples after 60 min of exposure to the effect of cavitation is shown in Fig. 5. With both materials, a more pronounced surface relief appeared. The thin surface layer is almost removed primarily by the separation of the glass beads. The removed layer is deeper in sample B where some residual ridges are visible (Fig. 5b)

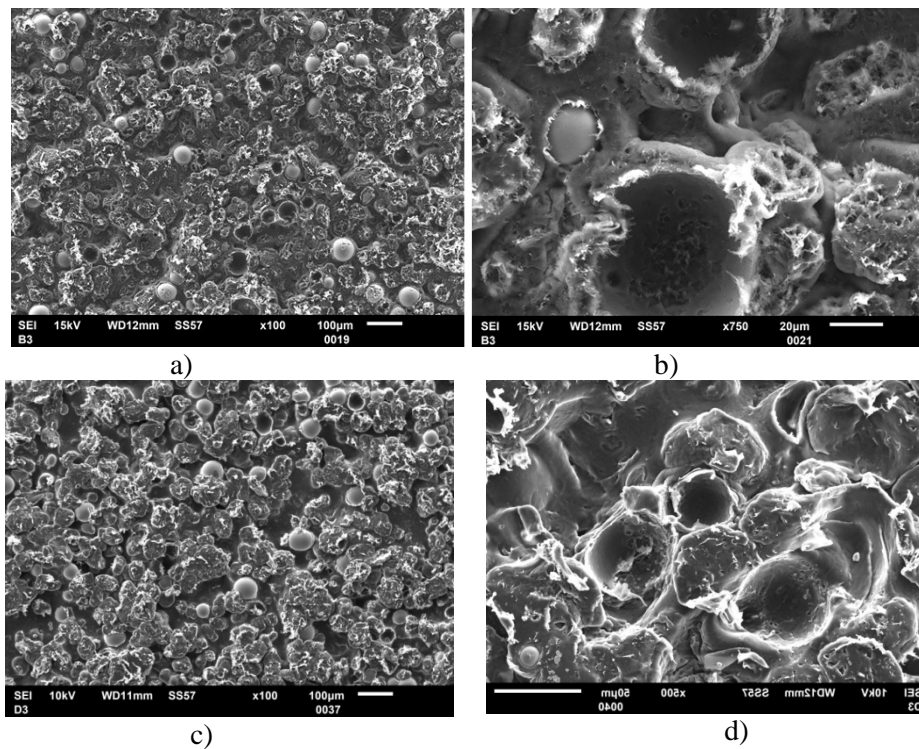


Fig. 6. Cavitation damage after 120 min of the PA 3200 GF materials: a) and b) A composite and c) and d) B composite.

After 120 min of cavitation testing, a significantly more severe damage may be observed, (Fig. 6). By comparing two tested materials, it can be noticed that the matrix of B composite becomes more brittle and the cracks propagate along the matrix rather than the particle /matrix interface (Fig.6b), compared to A composite (Fig. 6d).

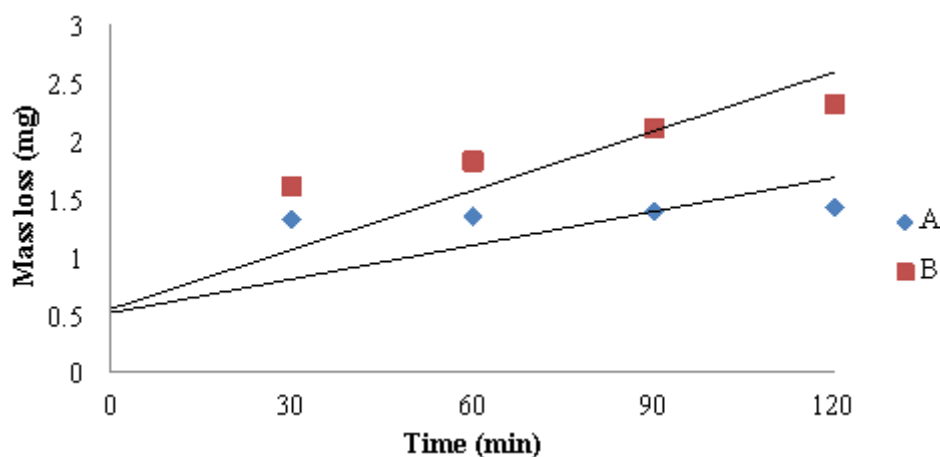


Fig. 7. Cavitation rate diagram of composite A and composite B.

The diagram in Fig. 7. presents relation between mass loss and testing time, where the line was drawn by the least-square method and data can be expressed by a straight line. The slope of the straight line represents the cavitation rate. The cavitation rates of A composite and B composite were calculated by dividing the total mass loss by the time of cavitation testing, in accordance with the ASTM G32 standard.

The material A, polyamide PA 3200 GF (glass bead filled polyamide 12 powder) - unused powder (100% new) show a lower cavitation rate ($V_A = 0.022$ mg/min) compared to composite B (recycled powder mixed with 70% of new powder), where the cavitation rate was higher ($V_B = 0.038$ mg/min) (Fig. 7).

4. Conclusion

The Polyamide powder PA 3200 GF reinforced with glass beads was produced by Selective laser sintering technology. The laser-sintered samples were produced from 100% new (Sample A) and recycled powder mixed with 70% of new powder (Sample B). The estimation of cavitation erosion of the composites using the ASTM G32 standard test revealed that both samples have good resistance to cavitation erosion. The morphology of the surface damage of the samples showed that the damage mechanism of samples A and B is the same. The difference is in the degree of damage, i.e. in the greater degree of surface roughness of sample B. This statement is also confirmed by the higher cavitation rate of sample B, i.e. its lower cavitation resistance.

Acknowledgments

This work was supported by the Ministry of Education, Science and Technological Development of the Republic of Serbia (Contracts No. 451-03-68/2022-14/200135, No. 451-03-68/2022-14/200213 and No. 451-03-68/2022-14/200108)

5. References

1. A. Pilipović, B. Valentan, T. Brajljih, T. Haramina, J. Balić, J. Kodvanj, M. Serčer, I. Drstvenšek, ICAT, DAAAM September, 22th – 24th, Nova Gorica, Slovenia, (2010)
2. A. Vranić, N. Bogojević, S. Ćirić Kostić, D. Croccolo, G. Olmi, IMK-14 – Research & Development in HM 23 (2017) 2 EN57-62.
3. A. A. Mousah, School of Engineering, Cardiff University United Kingdom, June (2011).
4. H. Unal, Materials & Design, 25 (2004) 483.
5. S. Hattori, E. Nakao, R. Yamaoka, T. Okada, Mechanical Engineers, Part A 65, (1999) 393.
6. R. T. Knapp, J.W. Daily, F. G. Hammit. Cavitation, New York: McGraw-Hill (1970).
7. T. Okada, Y. Iwai, S. Hattori, N. Tanimura, Wear 184 (1995) 231–239.
8. T. S. Shih, S. Y. Chau, C. H. Chang, AFS Trans, 96 (1988) 557.
9. S. Suslick, A. Crum, Handbook of acoustics, New York: Wiley (1994)
10. M. Pavlović, M. Dojčinović, R. Prokić-Cvetković, Lj. Andrić, Science of Sintering, 51 (2019) 410.
11. Durmuş, H., Gül, C., Çömez, N., & Uzun, R. From metal chips to composite, Science of Sintering, 52 (2) (2020) 178.
12. S. Kenneth Suslick, Y. Didenko, M. M. Fang, H. Taeghwan, J. K. Kolbeck, W. B. McNamara, M. M. Mdleleni, M. Wong, Jour. Philosoph. Trans. Roy. Soc. A: Mathem. Phys. & Eng. Science, 357 (1999) 335.
13. M. Dular, A. Osterman, Wear, 265 (2008) 811.
14. B. Dular, B. Bachert, B. Stoffel, Wear 257 (2004) 1176.
15. F. Wantang, Z. Yangzeeng, J. Tianfu, Y. Mei, Wear, 205 (1997) 28.
16. A. Terzić, M. Dojčinović, Lj. Miličić, J. Stojanović, Z. Radojević, Science of Sintering, 53 (2021) 445.
17. F. AbuSahmin, A. Algellai, N. Tomić, M. M., Vuksanović, J. Majstorović, T., Volkov Husović, V. Simić, R. Jančić Heinemann, M. Toljić, J. Kovačević, Science of Sintering, 52 (2020) 68.
18. Material data sheet PA 3200 GF, AHO / 01.09, EOS GmbH (2009).
19. Formiga P100. User Manual EOS; Formiga P100: Munich, Germany (2008).
20. Standard Method of Vibratory Cavitation Erosion Test, G32-92 Annual Book of ASTM Standards, Vol. 03.02. Philadelphia, ASTM (1992).
21. N. Sushant, R. K. Sharma, S. Dhiman, Mater. & Manufact. Proc., (2015) 3.

Сажетак: Ова студија је усредсређена на резултате истраживања отпорности на кавитацију узорака добијених технологијом селективног ласерског синтеровања. Узорци су израђени од полиамидног праха ојачаног стакленим честицама – PA 3200 GF. Ласерски синтеровани узорци произведени су од 100% новог и рециклираног праха помешаног са 70% новог праха. Узорци су испитивани у условима кавитације коришћењем методе ултразвучних вибрација са стационарним узорком према стандарду ASTM G32. Испитивање морфологије кавитационог оштећења испитивано је помоћу скенирајућег електронског микроскопа. Промена губитка масе током различитих времена кавитације мерена је на испитиваним узорцима. Основни циљ истраживања био је утврђивање валидности примене испитиваног материјала у условима кавитације.

Кључне речи: Полиамидни прах, PA 3200 GF; Морфологија; Брзина кавитације; Селективно ласерско синтеровање.

© 2023 Authors. Published by association for ETRAN Society. This article is an open access article distributed under the terms and conditions of the Creative Commons — Attribution 4.0 International license (<https://creativecommons.org/licenses/by/4.0/>).

